JTE HCMUTE
ISSN: 2615-9740

JOURNAL OF TECHNICAL EDUCATION SCIENCE
Ho Chi Minh City University of Technology and Education
Website: https://jte.edu.vn
Email: jte@hcmute.edu.vn

Fabrication of Bismuth Oxychloride / Reduced Graphene Oxide Composites for Visible-Driven Photocatalysis

Bao-Ngoc Nguyen-Thi[1], Thuy-An Nguyen-Thi[2], Quoc-Cuong Huynh[3], Kim Thi Nguyen[1], Thanh-Truc Pham[1*]

[1]Ho Chi Minh City University of Technology and Education, Vietnam
[2] La Party Corporation Vietnam Company Limited, Binh Duong Province, Vietnam
[3]KCC (Vietnam) Company Limited, Long Thanh Industrial Park, Dong Nai Province, Vietnam

[*]Corresponding author. *Email: trucpt@hcmute.edu.vn*

ARTICLE INFO

Received: 17/08/2024
Revised: 22/09/2024
Accepted: 25/10/2024
Published: 28/05/2025

KEYWORDS

Photocatalysis;
Bismuth oxychloride;
Reduced graphene oxide;
Rhodamine B;
Visible light.

ABSTRACT

In this study, the BiOCl/rGO (BR) nanocomposites were fabricated via different pathways, BiOCl nanocrystals were directly grown on graphene oxide (GO) sheets and BiOCl nanoflowers and GO were attached after individual fabricated. The reduction of GO was also carried out completely. The basic properties and structures of BiOCl and BiOCl/rGO were evaluated by convert infrared spectroscopy (FT-IR), X-ray diffraction spectroscopy (XRD), Raman scattering spectroscopy and scanning electron microscope (FE-SEM). In this case, the direct growth of BR performed stronger linkage between BiOCl and rGO through the chemical interaction of the Bi-C bond. The complex interaction between the optical and electrical factors of BR material has provided new opportunities to optimize the photocatalytic activity. BiOCl combined with rGO overcame the disadvantage of rapid recombination of electron-hole pairs, thereby enhancing the photocatalytic activity of the material. The results showed the improvement of reaction rate constant was 1.45 times higher than that of pristine BiOCl, which can totally remove rhodamine 10 ppm in 30 min.

Doi: https://doi.org/10.54644/jte.2025.1644

1. Introduction

Besides the speedy development of urbanization, lots of environmental contaminated problems have increased. More and more wastewater containing heavy metals, radionuclides and organic contaminants is discharged into natural environment. Therefore, it is fundamental to find a highly efficient and eco-friendly system to transform organic contaminants into harmless subtances, such as H_2O and CO_2 [1].

Photocatalysis is considered as a promising mechanism and generally applied for wastewater filtration. Bismuth oxychloride (BiOCl) photocatalyst has attracted special attention because of its lofty chemical balance, great photoluminescence properties and low toxicity. Thus, the BiOCl photocatalyst had been effectively utilized environmental treatment. In the structure of BiOCl, each [Cl–Bi–O–Bi–Cl] had a Bi atom coordinates with four surrounding Cl atoms and four O atoms to make a conical decahedral structure with divergent orientations and upper and lower asymmetry. Furthermore, BiOCl is a p-type semiconductor and the wide band gap stimulated by UV light [2].

Nevertheless, the wide band gap energy (Eg = 3.4 eV) and the fast recombination rate of electrons and holes are two disadvantages of BiOCl. Currently, many different methods have used to repair those disadvantages, such as surface modification, doping, morphology and incorporation control [3]. Graphene has attracted scientific interest over the past decade because of its outstanding properties. However, plenty of methods use strong oxidants, causing some significant defects in the crystal lattice of GO. Fortunately, the GO can recover graphene-like properties by converting GO into rGO. At this moment, the rGO is becoming a good adjustment between GO and graphene [4]–[6].

This study focuses on the synthesis of BiOCl/rGO composite. The addition of rGO to BiOCl prevents recombination of electron-hole pairs, narrows the band gap, reduces crystalline size, and improves absorption in the visible light region. It is expected that BiOCl/rGO will be able to produce photocatalytic reactions with higher efficiency than the pristine BiOCl.

Figure 1. *GO suspension*.

2. Materials and Methods

2.1. Materials

Bismuth nitrate pentahydrate $Bi(NO_3)_3.5H_2O$ 99.8%, thiourea (TU) and potassium chloride were purchased from Sigma (Germany). Ethanol absolute and potassium permanganate (KMnO4) originated from VN-Chemsol (Vietnam). Acetic acid, ethylene glycol, graphite powder, phosphoric acid (H_3PO_4), sulfuric acid (H_2SO_4), hydrogen peroxide (H_2O_2), hydrochloric acid (HCl) and ascorbic acid (Vitamin C) originated from Xilong (China). Rhodamine B (RhB) originated from Oxford Lab (India).

2.2. Characterizations

The crystal structure of the samples was inspected using X-ray diffraction (XRD, Empyrean – PANalytical) with Cu-Kα radiation (λ = 1.54 Å). The morphology and microstructure of the samples were analyzed using field emission scanning electron microscopy (FE-SEM, Regulus 8100, Hitachi). Functional groups were determined using Fourier-transform infrared spectroscopy (FT-IR, Nicolet 6700, Thermo). Bandgap widths were analyzed using UV diffuse reflectance spectroscopy (DRS, V-570 UV/VIS, Jasco). Light absorption efficiency was evaluated using UV-Vis absorption spectroscopy (CRF - V-730, Jasco). The chemical structure of the samples was analyzed using Raman spectroscopy (Xpolra Plus, Horiba).

2.3. Methods

2.3.1. Synthesis of graphene oxide (GO)

The Hummer's method was used to synthesize GO as follows: 0.225 g of graphite powder was mixed in 30 mL of H2SO4:H3PO4 (9:1 v/v) mixed solvent under gently stirring. The mixture was then transferred an ice bath, and 1.32 g of $KMnO_4$ was mixed slowly into the mixture. The above solution

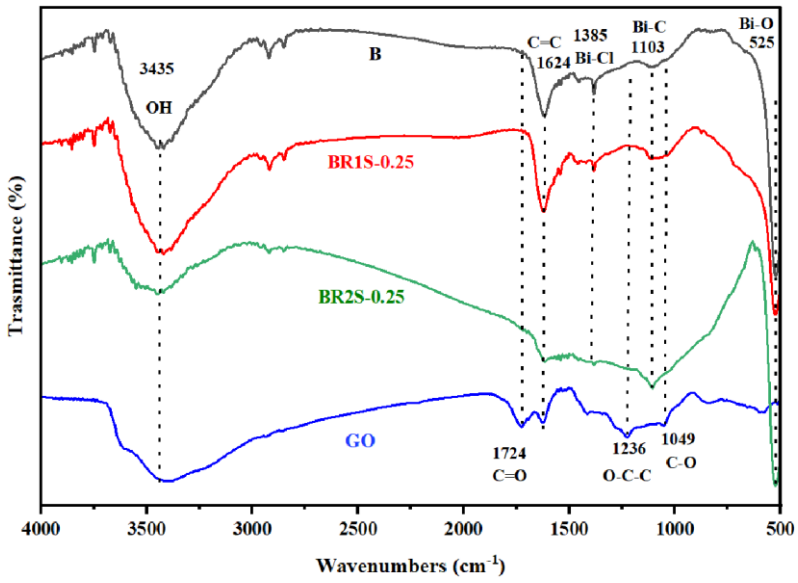

Figure 2. *FT-IR spectra of samples.*

was dispersed for 6 hours until the color turned into dark green. After that, 0.675 ml of H_2O_2 was added dropwise and stirred for 10 min to remove excess $KMnO_4$. The exothermic reaction occurred and furthered by cooling down to room temperature [7]. 30 ml of deionized water and 10 ml of HCl 10% were added and centrifuged at 4000 rpm for 10 minutes. Next, the supernatant was transferred away and the residuals was centrifuged and washed with DI water. Finally, the obtained product is GO in gel form as shown in **Figure 1**.

2.3.2. Synthesis of BiOCl

BiOCl nanoparticles, denoted as B, were prepared by a sol gel method. Firstly, 50 ml of a solution of ethylene glycol and distilled water (1:1 v/v) was prepared as a solvent mixture. Then, 0.005 mol bismuth nitrate pentahydrate ($Bi(NO_3)_3.5H_2O$) was mixed into the solvent mixture, followed by a constant stirring for about 30 min. After well mixed, 0.005 mole of thiourea was added. When a white suspension appeared, 0.005 mole of potassium chloride would be introduced to the reaction. 50 ml of 2 % acetic acid solution was then slowly dropwised into the above mixture, followed by a vigorous stirring for 1h at 25 ^{0}C. Finally, the samples were washed and separated with distilled water by filtration a few times and dried at 60 ^{0}C for 12 h [8].

2.3.3. Synthesis of BiOCl/rGO by in-situ method

The GO suspension was added in 25 mL deionized water and dispersed by ultrasonication. After 30 min, 25 ml of EG was mixed in the above mixture, then the mixture was further stirred for 30 min at 25 °C to form the GO mixture. In the following step, 0.005 mol $Bi(NO_3)_3.5H_2O$ was dispersed into the aforementioned mixture by vigorously stirring at 25 °C to a homogeneous mixture. The following steps were then conducted as the BiOCl process. After washing with distilled water, ascorbic acid was added into the mixture at a ratio of (0,02 g/30 ml) in order to reduce GO into rGO. After being stirred for 20 min at 70 °C, the product was washed with DI water and dried at 60 °C for 12 h. The samples were denoted as BR1S-*x*, where *x* = 0.25, 0.5, 5, 7, 10, 15 wt% is the GO content.

2.3.4. Synthesis of BiOCl/rGO by ex-situ method.

In this case, the composites were formed through a hydrothermal process. At first, 0.03 g of GO suspension was added in 30 ml ethanol:distilled water (1:2 v/v) mixed solvent under ultrasonic treatment for 30 min. Then, 0.06 g B was dissolved into the above mixture. After stirring for 2 h, the mixture placed into a 100 ml Teflon-lined stainless-steel autoclave and treated at 160 °C for 3 h, when the heat will reduce the oxygen-containing functional groups in GO to form rGO. The sample was then naturally cooled to 25 °C. The product was separated by filtration, washed with distilled water and dried at 80 °C for 4 h. Finally, the photocatalyst was grinded as powder and named as BR2S-*x*, where *x* = 0.25, 0.5, 5, 7, 10, 15 wt% is the GO content.

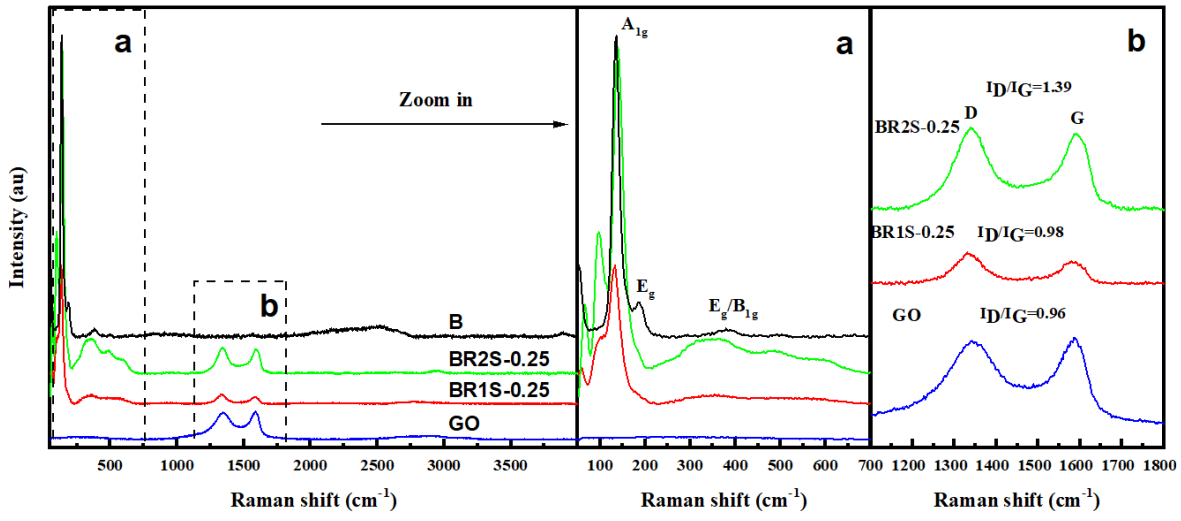

Figure 3. *Typical Raman spectra of B, BR-1S, BR-2S and GO.*

3. Results and Discussions

3.1. Characterizations

The vibrations of typical functional groups on the photocatalyst are shown in **Figure 2**. The FTIR spectra of BiOCl, GO and BiOCl/rGO composites (BR) performed similar absorption bands at 3426 cm^{-1} and 1623 cm^{-1}, which related to the stretching vibration of O-H in absorbed water and C=C. In the spectrum of GO, signals at 1724 cm^{-1}, 1049 cm-1 and 1236 cm-1 were assigned to stretching vibration of C=O, C-O and C-O-C. Nevertheless, the characteristic peaks of GO at 1725 cm^{-1}, 1226 cm^{-1} and 1052 cm^{-1} were completely absent in BR1S-0.25 and BR2S-0.25, indicating the ability to remove oxygen-containing functional groups, in the other word, successfully reduction of GO to rGO by either vitamin C or thermal reduction processes. The bands at 1383 cm^{-1} and 524 cm^{-1} were corresponded to stretching vibrations of Bi-Cl and Bi-O, which could be observed in both B and BR1S-0.25 and BR2S-0.25. Moreover, The FTIR spectrum of BR at 1113 cm^{-1} was related to Bi-C band, which demonstrated for the chemical interaction between BiOCl and rGO [3].

The chemical structure of BiOCl/rGO was analyzed by Raman spectroscopy. The Raman spectra of B exhibited the strong peak at 136 cm^{-1} was corresponded to the A_{1g} internal Bi-Cl stretching vibration, and the peak at 187 cm^{-1} was related to the E_g internal Bi-Cl stretching vibration (see **Figure 3**). However, in the BR composites, it can be seen that the A_{1g} peak becomes lower intensity and broader, whereas the E_g peak seems to have disappeared when incorporated with rGO. Furthermore, there was a broad weak band at 389 cm^{-1} corresponded to the E_g/B_{1g} modes originated from the movement of the oxygen atoms.

Two distinctive bands at 1601 cm^{-1} and 1344 cm^{-1} belonging to the G and D bands of graphene were observed in the Raman spectra of GO. Nevertheless, in the BiOCl/rGO composites, due to the chemical interaction between BiOCl and rGO, the G and D moved towards 1333 cm^{-1} and 1585 cm^{-1}. The I_D/I_G ratio is 0.96 for GO, 1.39 for BR1S-0.25 and 0.98 for BR2S-0.25. Compared with GO, the I_D/I_G ratio of rGO is higher. It is shown that the average size of sp^2 domains decreases after GO reduction of GO owing to the removal of oxygen- containing functional groups by hydrothermal treatment and vitamin C. Reduction of GO causes fragmentation throughout the reactive sites, generating new graphitic domains as well as a great deal of edges that act as defects, growing the D peak [9].

The XRD patterns of as-prepared the composites and pure BiOCl are given in **Figure 4**. The diffraction peaks (2θ) at 11.92^0, 24.15^0, 25.94^0, 32.58^0, 33.45^0 and 46.76^0 correspond to the (001), (002), (101), (110), (102) and (200) diffraction planes of BiOCl (JCPDS 06-0249). These signals perform sharp

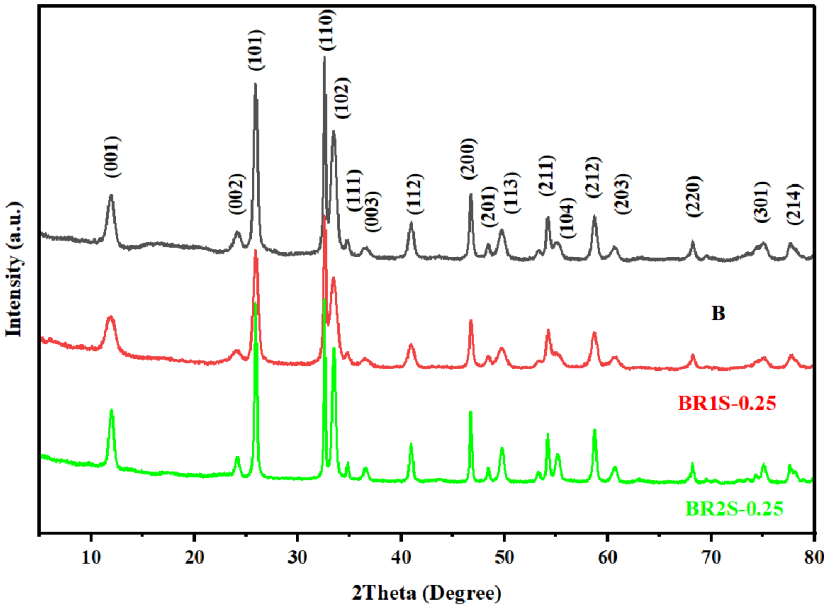

Figure 4. *XRD pattern of BiOCl and composite samples.*

JTE
HCMUTE
ISSN: 2615-9740

JOURNAL OF TECHNICAL EDUCATION SCIENCE
Ho Chi Minh City University of Technology and Education
Website: https://jte.edu.vn
Email: jte@hcmute.edu.vn

Table 1. *Crystalline sizes of B, BR1S-0.25 and BR2S-0.25 calculated by Scherrer's equation* $D = \frac{k\lambda}{\beta cos\theta}$.

Series	β (°)	2θ (°)	D (*nm*)
B	0.270	32.589	32.091
BR1S-0.25	0.313	32.594	27.669
BR2S-0.25	0.198	32.589	43.621

shape and strong intensity in all of the samples, which indicates the high crystallinity of the BiOCl phase [10]–[12]. The diffraction peak of BR2S was sharper and narrower than that of B, indicating that BR2S had better crystallinity and larger crystalline size than B. However, the lower intensity and wider diffraction peak of BR1S compared to B demonstrate the introduction of graphene reduced the crystallinity of BR1S, the material produced more crystals and smaller crystalline size. Additionally, the typical diffaction peak of rGO at 2θ=26° did not appear in the XRD spectra of the composites. This could be due to the concentration of rGO being too small to be detected [13], [14].

According to **Table 1**, the crystalline size of samples B, BR1S-0.25 and BR2S-0.25 are 32.091nm, 27.669nm and 43.621nm, respectively. The sample BR1S was decreased in size as compared to B. The decrease in size of BR1S can be explained by the attraction of bismuth complex in the "sol" by the oxygen-containing groups on the surface of GO during the praparation process. The concentrated of complex in these positions would create more crystal nuclei than just the original BiOCl, so the amount of crystal nuclei is greater when growing, the crystalline size is smaller, which is in consistent with the previously analyzed XRD results.

As shown in **Figure 5a**, BiOCl had a flower-like structure, with a fairly uniform shape, size and density. The thickness of the nanosheet is about 23.8 nm. **Figure 5b-c** displayed SEM images of BR1S-0.25 and BR2S-0.25. In **Figure 5b**, the BiOCl sheets agglomerated into flower-like blocks, whereas rGO were completely covered by these flowers and unobservable by SEM. On the contrary, the sample BR2S-0.25 expressed that the rGO sheets were evenly wrapped onto the surface of the BiOCl, making it difficult to see whether there is the flower-like structure. Such morphology leads to the reduction of surface area, which is indirectly negatively affected to the photocatalytic efficiency.The optical properties of B, BR1S-0.25 and BR2S-0.25 were analyzed by UV-vis diffuse reflectance spectroscopy (DRS). In **Figure 6a**, the composite demonstrated broader absorption in the ultraviolet and visible regions compared with the narrow absorption of BiOCl in ultraviolet region with the light edge at 372 nm. The maximal absorbance wavelengths of BR2S-0.25 and BR1S-0.25 were 378 and 387 nm, respectively. The absorption ability of BiOCl/rGO was improved due to rGO acting as an electron reservoir to trap electrons under irradiation, thus expected to provide better photocatalytic performance.

The band gap energy of all the samples can be estimated by the Tauc plot: $h\nu = A\,(h\nu - E_g)^{n/2}$ where ν, α, A and E_g represent the light frequency, absorption coefficient, a constant and band gap energy respectively. For BiOCl, n is 1/2 due to its indirect transition [8], [11]. In **Figure 6b-d**, the band gap energy of B, BR1S-0.25 and BR2S-0.25 were 2.81 eV, 2.67 eV and 2.77 eV, respectively. The

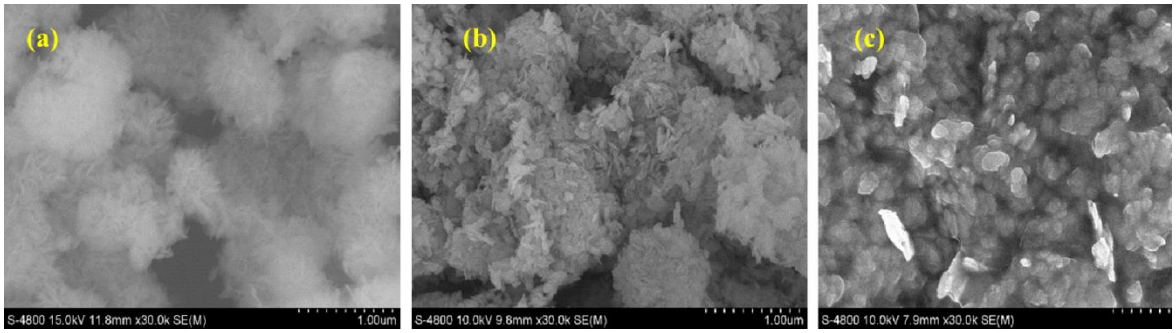

Figure 5. *FE-SEM images (a) sample B, (b) sample BR1S-0.25, (c) sample BR2S-0.25*

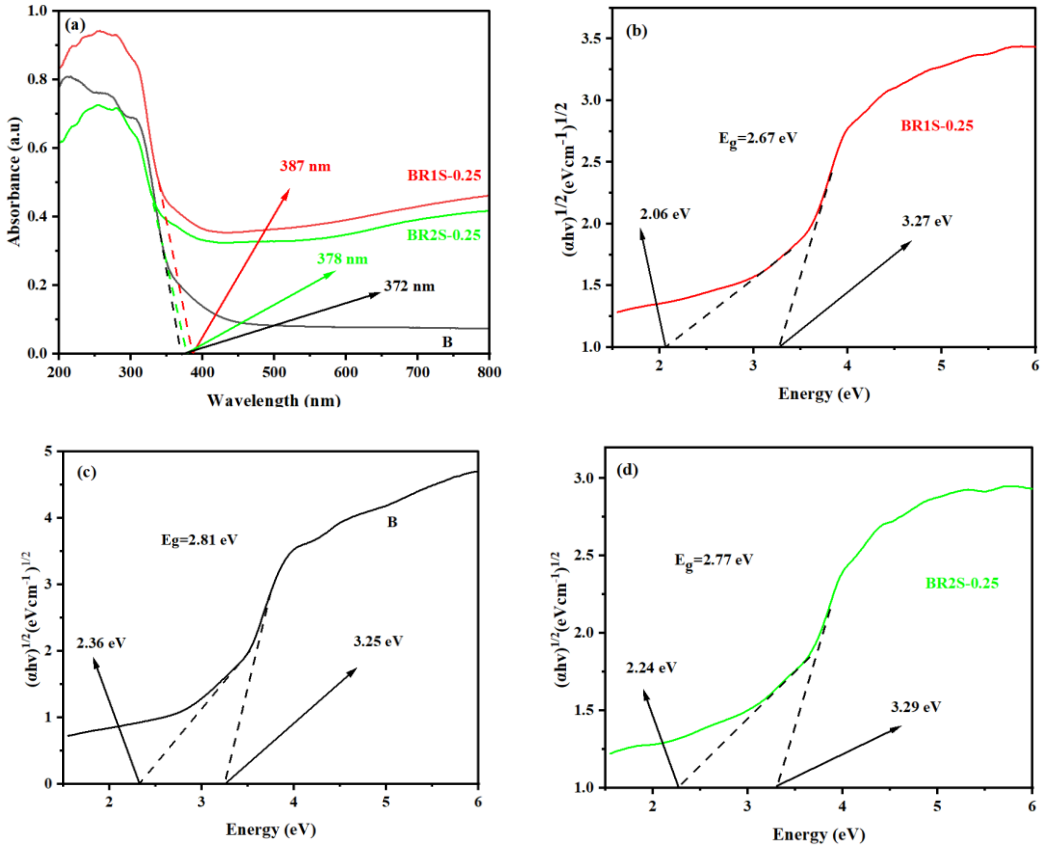

Figure 6. *(a) UV–Vis diffuse reflectance spectra of samples B, BR1S-0.25, BR2S-0.2.5; plots of $(\alpha hv)^{1/2}$ versus hv of (b) BR1S-0.25, (c) B, (d) BR2S-0.25 samples.*

composites had lower band gap energy than B, indicating greater optical absorption ability in the ultraviolet and visible light regions. This result may be due to the chemical interaction of the Bi-C band between BiOCl and rGO, suggesting the possibility of more excited electrons and thus expected enhancement of photocatalytic activity [3].

3.2. Photocatalytic performances of the BiOCl/rGO composites.

As shown in **Figure 7f**, after the photocatalytic process, the maximum absorption intensity at 554 *nm* gradually decreased shows that most of RhB was completely decomposed during the photocatalytic process. In **Figure 7a-e**, the BR1S-0.25 photocatalyst achieves high degradability of 99.29% for the photodegradation of RhB after 30 minutes of irradiation, bringing about k_{app} = 0.1059 min^{-1} in reaction rate constant. In the ex-situ method, once again the finest rGO concentration is 0.25 wt%, which can remove 99.24% of RhB in 30 min and k_{app} = 0.0661 min^{-1}. Yet, the difference in rate constant between BR1S-0.25 and BR2S-0.25 indicates an excellent in-situ association effect between BiOCl and rGO. As for the references, the k_{app} = 0.7032 min^{-1} is observed for pristine BiOCl, underlying the rationality of the in-situ method. This result is consistent with the DRS analysis results for the band gap, the band gap of BR1S-0.25 is the smallest so the RhB decomposition rate is fast. Additionally, the incorporation of rGO reduces the size of the BiOCl nanosheets, leading to an increase in the contact area and narrowing the band gap of the material, helping to improve the photocatalytic activity of B.

The k_{app} value shows that the appearance of GO plays an important role in charge transfer, increasing photocatalytic efficiency. Likewise, high concentration of rGO inhibited the interaction BiOCl/rGO composite to interact with visible light, resulting in reduced photocatalytic activity [15]. The concentration of rGO might have been increased, the rGO particles hindered the interaction of BiOCl with RhB solution so the reaction rate decreased. Otherwise, it's also possible that rGO competed with

BiOCl in absorbing light, reducing the amount of light reaching the surface of BiOCl and affecting the reaction rate.

4. Conclusions

In this study, BiOCl/rGO composite materials have been successfully synthesized using in-situ and ex-situ methods. SEM and XRD analysis results show that the formation of a sheet-like structure of small BiOCl nanocrystals randomly grown on the surface of GO, strongly indicates the interaction between BiOCl and rGO. The BR1S-0.25 has the highest photocatalytic activity under visible light irradiation for RhB decomposition. The increased photocatalytic reaction rate constant is mainly due to the small size of the BiOCl nanosheets, the chemical bonds between rGO and BiOCl beneficial for charge transferring, thus improving the efficiency of electron and hole separation.

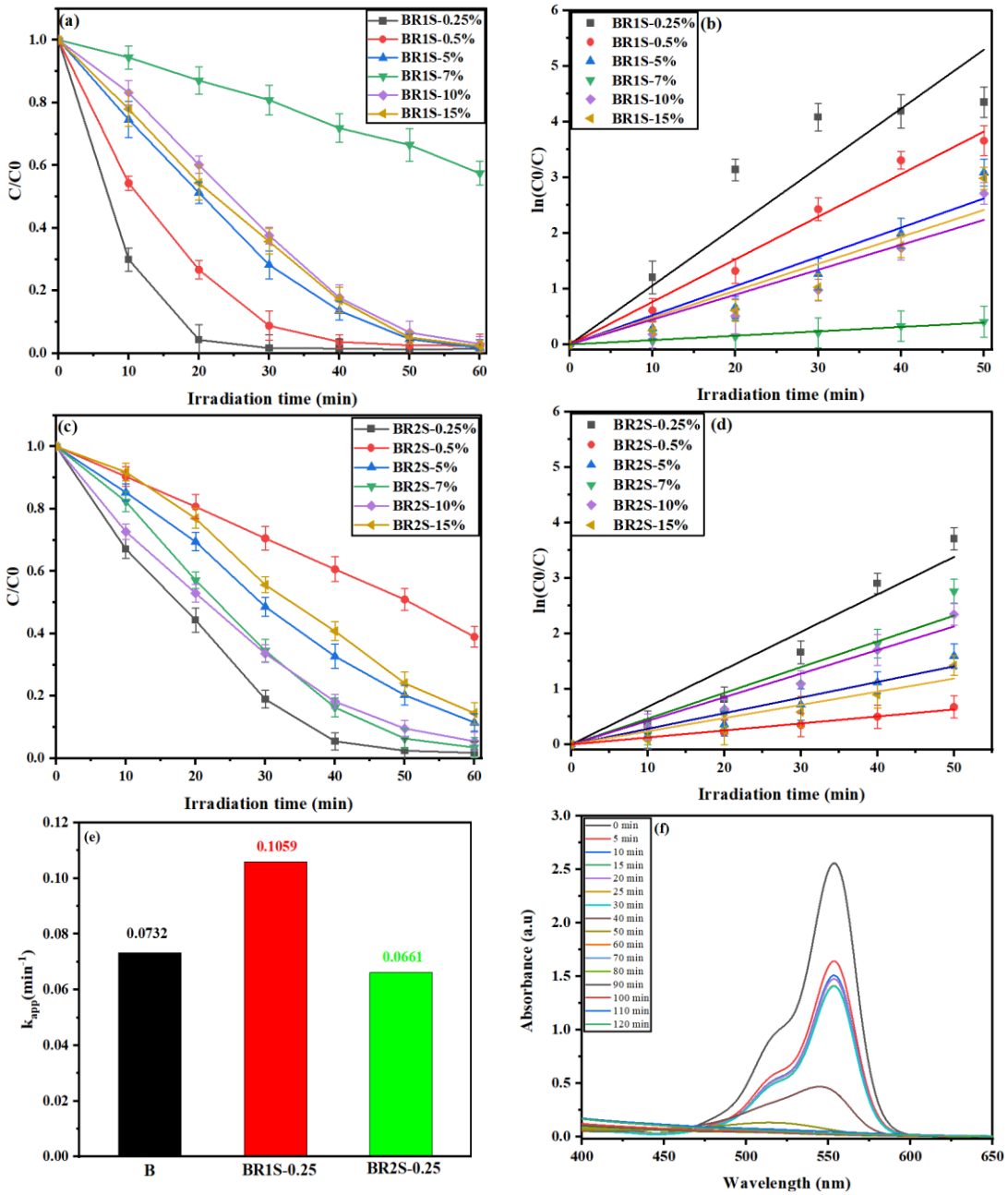

Figure 7. *(a, c) The removal of RhB; (b, d) Kinetic plots show the photocatalytic degradation of RhB 10 ppm within 50 min over BR1S-x and BR2S-x, respectively; (e) The reaction rate constant k_{app} of BR1S-x and BR2S-x; (f) UV-Vis absorption spectra of sample BR1S-0.25.*

Acknowledgments

This work belongs to the project SV2024-36 funded by the Ho Chi Minh City University of Technology and Education, Vietnam.

Conflict of Interest

The authors declare no conflict of interest.

REFERENCES

[1] L. Yao, H. Yang, Z. Chen, M. Qiu, B. Hu, and X. Wang, "Bismuth oxychloride-based materials for the removal of organic pollutants in wastewater," *Chemosphere*, vol. 273, p. 128576, 2021.
[2] W. W. Liu and R. F. Peng, "Recent advances of bismuth oxychloride photocatalytic material: Property, preparation and performance enhancement," *J. Electron. Sci. Technol.*, vol. 18, no. 2, p. 100020, 2020.
[3] J. Zhang *et al.*, "Ultra-light and compressible 3D BiOCl/RGO aerogel with enriched synergistic effect of adsorption and photocatalytic degradation of oxytetracycline," *J. Mater. Res. Technol.*, vol. 8, no. 5, pp. 4577–4587, 2019.
[4] R. Tarcan, O. T. Boer, I. Petrovai, C. Leordean, S. Astilean, and I. Botiz, "Reduced graphene oxide today," *J. Mater. Chem. C*, vol. 8, no. 4, pp. 1198–1224, 2020.
[5] A. T. Smith, A. M. LaChance, S. Zeng, B. Liu, and L. Sun, "Synthesis, properties, and applications of graphene oxide/reduced graphene oxide and their nanocomposites," *Nano Mater. Sci.*, vol. 1, no. 1, pp. 31–47, 2019.
[6] J. Phiri, P. Gane, and T. C. Maloney, "General overview of graphene: Production, properties and application in polymer composites," *Mater. Sci. Eng. B*, vol. 215, pp. 9–28, 2017.
[7] N. I. Zaaba, K. L. Foo, U. Hashim, S. J. Tan, W. W. Liu, and C. H. Voon, "Synthesis of graphene oxide using modified hummers method: solvent influence," *Procedia Eng.*, vol. 184, pp. 469–477, 2017.
[8] J. Hou *et al.*, "Narrowing the band gap of BiOCl for the hydroxyl radical generation of photocatalysis under visible light," *ACS Sustain. Chem. Eng.*, vol. 7, no. 19, pp. 16569–16576, 2019.
[9] M. R. Martínez, M. A. Álvarez, M. V. L. Ramón, G. C. Quesada, J. R. Utrilla, and M. S. Polo, "Hydrothermal synthesis of rGO-TiO_2 composites as high-performance UV photocatalysts for ethylparaben degradation," *Catalysts*, vol. 10, no. 5, p. 520, 2020.
[10] J. Xiong, G. Cheng, G. Li, F. Qin, and R. Chen, "Well-crystallized square-like 2D BiOCl nanoplates: mannitol-assisted hydrothermal synthesis and improved visible-light-driven photocatalytic performance," *RSC Adv.*, vol. 1, no. 8, pp. 1542–1553, 2011.
[11] T. D. Puttaraju *et al.*, "The evaluation of various biological properties for bismuth oxychloride nanoparticles (BiOCl NPs)," *Inorg. Chem. Commun.*, vol. 144, p. 109850, 2022.
[12] W. Lin *et al.*, "Carbon dots/BiOCl films with enhanced visible light photocatalytic performance," *J. Nanoparticle Res.*, vol. 19, pp. 1–11, 2017.
[13] F. Q. Li *et al.*, "Enhanced photocatalysis performance of BiOCl/graphene modified via polyvinylpyrrolidone," *Vacuum*, vol. 184, p. 109857, 2021.
[14] M. Bera, P. Gupta, and P. K. Maji, "Facile one-pot synthesis of graphene oxide by sonication assisted mechanochemical approach and its surface chemistry," *J. Nanosci. Nanotechnol.*, vol. 18, no. 2, pp. 902–912, 2018.
[15] C. Y. Wang, T. Wu, and Y. W. Lin, "Preparation and characterization of bismuth oxychloride/reduced graphene oxide for photocatalytic degradation of rhodamine B under white-light light-emitting-diode and sunlight irradiation," *J. Photochem. Photobiol. A Chem.*, vol. 371, pp. 355–364, 2019.

Nguyen Thi Bao Ngoc received the B.S from the Ho Chi Minh City University of Technology and Education, Ho Chi Minh City, Vietnam, in 2024. She interned at Tang Long Pack Company Limited, Ho Chi Minh City, Vietnam, in 2023. Her research interests include photocatalytic chemical reactions, photocatalysts based on semiconductor materials and composites of semiconductor-polymeric materials.
Email: 20130047@student.hcmute.edu.vn. ORCID: https://orcid.org/0009-0004-3664-6468

Nguyen Thi Thuy An received the B.S from the Ho Chi Minh City University of Technology and Education, Ho Chi Minh City, Vietnam, in 2023. Currently, she is working in the quality control of La Party CORPORATION Vietnam Co., Ltd. Her research interests include photocatalytic chemical reactions, photocatalysts based on semiconductor materials and composites of semiconductor-polymeric materials.
Email: vnlaparty1@gmail.com ORCID: https://orcid.org/0009-0000-4648-8695

Huynh Quoc Cuong received the B.S. from the Ho Chi Minh City University of Technical Education, Ho Chi Minh City, Vietnam, in 2024. Currently, she is working in KCC (Vietnam) Company Limited. His research interests include photocatalytic chemical reactions, semiconductor-based photocatalysis, and semiconductor-polymer composite materials.
Email: quoccuong24042001@gmail.com .ORCID: https://orcid.org/0009-0002-3120-4260

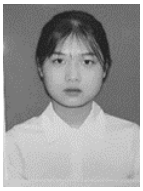

Nguyen Kim Thi received the B.S. from the Ho Chi Minh City University of Technical Education, Ho Chi Minh City, Vietnam, in 2024. She has been working in the Quality Engineering department through her internship at Sailun Group, Vietnam. Her research interests include photocatalytic chemical reactions, semiconductor-based photocatalysis, and semiconductor-polymer composite materials.

Email: 20130040@student.hcmute.edu.vn. ORCID: https://orcid.org/0009-0004-3793-6299

Pham Thanh Truc received the B.S. from the Ho Chi Minh City University of Technology, Ho Chi Minh City, Vietnam, in 2013, and the M.S-Ph.D. intergrated degree from the School of Chemical Engineering, University of Ulsan, Ulsan, South Korea, in 2018. She is currently a Lecturer with the Department of Materials Technology, Ho Chi Minh City University of Technology and Education (HCMUTE), Vietnam. Her research interests include photocatalytic chemical reactions, photocatalysts based on semiconductor materials and composites of semiconductor-polymeric materials. intelligent control, nonlinear control, modern control theories, and their applications in robotics.

Email: trucpt@hcmute.edu.vn. ORCID: https://orcid.org/0000-0003-3958-4878